

# Fast electron spin flips via strong subcycle electric excitation

Máté Tibor Veszeli<sup>1</sup> and András Pályi<sup>2</sup>

<sup>1</sup>*Institute of Physics, Eötvös University, 1518 Budapest, Hungary*

<sup>2</sup>*MTA-BME Exotic Quantum Phases "Momentum" Research Group and Department of Physics, Budapest University of Technology and Economics, 1111 Budapest, Hungary*

An important goal in quantum information processing is to reduce the duration of quantum-logical operations. Motivated by this, we provide a theoretical analysis of electrically induced fast dynamics of a single-electron spin-orbit qubit. We study the example of a one-dimensional quantum dot with Rashba spin-orbit interaction and harmonic driving, and focus on the case of strong driving, when the real-space oscillation amplitude of the driven electron is comparable to the width of its wave function. We provide simple approximate analytical relations between the qubit Larmor frequency, the shortest achievable qubit-flip time, and the driving amplitude required for the shortest achievable qubit flip. We find that these relations compare well with results obtained from numerical simulations of the qubit dynamics. Based on our results, we discuss practical guidelines to maximize speed and quality of electric single-qubit operations on spin-orbit qubits.

PACS numbers:

## I. INTRODUCTION

An important physical quantity in quantum information processing is the speed of single-qubit logical operations. Often the quality of a certain physical qubit realization is characterized by the ratio between the decoherence time and the time required to perform coherent operations; the larger this ratio (quality factor), the better the qubit. Motivated by this, here we theoretically study a way to minimize single-qubit gate times for single-electron spin-orbit qubits in quantum dots<sup>1–8</sup>. More precisely, we investigate how spin-orbit-mediated qubit-flip processes can be made fast using short pulses of intense ac electric fields, with a pulse length comparable to the driving period.

We will consider harmonic electric driving, described by the Hamiltonian

$$H_E(t) = eE_{ac}z \sin(\omega t), \quad (1)$$

where  $e$  is the elementary charge,  $E_{ac}$  is the amplitude of the driving electric field,  $z$  is a spatial coordinate, and  $\omega$  is the driving (angular) frequency. We will consider the situation when the qubit is in its ground state at  $t = 0$ , driving starts at  $t = 0$ , and is stopped at  $t = \tau$ ; we call  $\tau$  the pulse duration. A constraint we introduce is that  $\omega\tau = N\pi$ ; that is, the pulse duration is an integer number of half-cycles. This constraint comes from a practical consideration: if driving is stopped at some arbitrary  $\tau$ , then the resulting electronic state at  $t = \tau$  could be very different from the eigenstates of the static Hamiltonian, and therefore be subject to significant time evolution even after the driving is stopped. We introduce the above constraint  $\tau = N\pi/\omega$  to avoid such a complication. This also implies that the shortest pulse in this framework corresponds to a single half-cycle of the excitation, that is,  $N = 1$  and pulse duration  $\tau = \pi/\omega$ , as shown in Fig 1b. This is the case we focus on.

The main question we address in this work is the following. Assume that certain practical constraints regard-

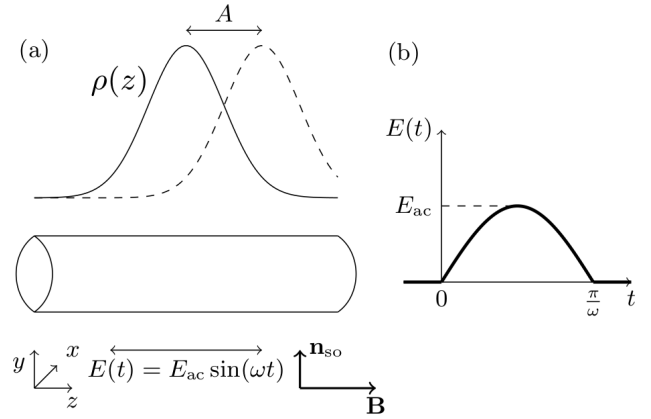


FIG. 1. **Half-cycle excitation of a one-dimensional spin-orbit qubit.** (a) A spin-orbit qubit is defined in a one-dimensional nanowire (cylinder), in the presence of a magnetic field  $\mathbf{B}$  and spin-orbit interaction, the latter characterized by the spin-orbit field direction  $\mathbf{n}_{so}$ . In equilibrium, the electron occupies the ground state, with charge density  $\rho(z)$ . Upon electric excitation  $E(t)$ , the electron is moved back and forth with amplitude  $A$  along the wire, inducing dynamics between the spin-orbit qubit basis states. (b) A half-cycle excitation: an appropriately tuned strong but short half-cycle excitation pulse induces a fast flip of the spin-orbit qubit.

ing the system parameters are given. Under those constraints, how fast can we perform a single qubit flip? What is the corresponding driving strength  $E_{ac}$  we have to apply to the system to achieve that fast qubit-flip? How do those quantities depend on the experimentally tunable parameters, such as the magnetic field strength and the spin-orbit interaction strength? We answer these questions within a specific model, and use those answers to establish practical guidelines for maximizing speed and quality of electric single-qubit operations on spin-orbit qubits.

In particular, the key findings within our model are

as follows. (i) We estimate that a fast qubit flip can be performed within 10 ps using a strong half-cycle pulse, assuming that the strong pulse does not ionize the quantum dot (see Section IV). (ii) The qubit flip can be made faster by increasing the external magnetic field  $B$ , and correspondingly increasing the drive frequency  $\omega$ , without the need of increasing the drive strength  $E_{ac}$  (see Section IV, Section VI, and Fig. 3). (iii) Counterintuitively, decreasing the strength of the spin-orbit interaction might allow for a faster qubit flip, although that requires an increased drive strength (see Section VII).

## II. SETUP

We examine a one-dimensional quantum dot, see Fig. 1a, described by the Hamiltonian

$$H(t) = H_{\text{osc}} + H_{\text{so}} + H_Z + H_E(t). \quad (2)$$

Here,  $H_{\text{osc}}$  is the harmonic oscillator term, that, is we approximate the confining potential with a parabola:

$$H_{\text{osc}} = \frac{p_z^2}{2m} + \frac{m\omega_0}{2} z^2 = \hbar\omega_0 \left( a^\dagger a + \frac{1}{2} \right), \quad (3)$$

where  $p_z = -i\hbar\partial_z$ , and  $a, a^\dagger$  are the ladder operators. The width of the oscillator ground-state wave function is  $L = \sqrt{\hbar/(m\omega_0)}$ . The electron is in a  $z$ -directional homogeneous magnetic field, which causes a Zeeman splitting between the spin-up and spin-down states, described by

$$H_Z = -\frac{g^*}{2} \mu_B B \sigma_z = -\frac{1}{2} \tilde{B} \sigma_z. \quad (4)$$

Here,  $B$  is the magnetic field strength,  $\mu_B$  is the Bohr-magneton,  $g^*$  is the effective  $g$ -factor and  $\sigma_z$  is the third Pauli matrix. The magnetic field points to the  $z$  direction. In this setup, electric spin control is enabled by spin-orbit coupling:

$$H_{\text{so}} = \alpha p_z \mathbf{n}_{\text{so}} \cdot \boldsymbol{\sigma} = \alpha p_z \sigma_y = i\tilde{\alpha} (a^\dagger - a) \sigma_y, \quad (5)$$

where  $\alpha$  is the Rashba spin-orbit coupling strength. The direction of the spin-orbit field is given by the unit vector  $\mathbf{n}_{\text{so}}$ , which we choose to be along the  $y$  direction, as shown in Fig. 1a. The electric driving has already been introduced in Eq. (1). With ladder operators it is expressed as:

$$H_E(t) = \tilde{E}_{ac} \sin(\omega t) (a^\dagger + a). \quad (6)$$

Note that we will consider cases when this electric driving is adiabatic with respect to the oscillator level spacing,  $\omega \ll \omega_0$ . In that case, the driving induces spatial oscillations of the electronic wave packet with an approximate amplitude  $A = \frac{\sqrt{2}\tilde{E}_{ac}}{\hbar\omega_0} L$ , as shown in Fig. 1a.

The quantities with tilde all have energy dimension, hence we can use them to compare the strengths of the different terms of the Hamiltonian; their definitions are

$$\tilde{B} = g^* \mu_B B, \quad (7a)$$

$$\tilde{\alpha} = \alpha \sqrt{\frac{m\hbar\omega_0}{2}}, \quad (7b)$$

$$\tilde{E}_{ac} = eE_{ac} \sqrt{\frac{\hbar}{2m\omega_0}}. \quad (7c)$$

The basis states of the spin-orbit qubit are the ground and first excited states of the static Hamiltonian  $H_{\text{osc}} + H_Z + H_{\text{so}}$ , to be denoted by  $|g\rangle$  and  $|e\rangle$ , respectively.

## III. QUBIT DYNAMICS AT WEAK DRIVING

Here, we outline the derivation leading to the weak driving results for the Larmor and the Rabi frequency<sup>5-8</sup>. Even though these results are already known, we include them here for self-containedness and to set the stage for our further results. The parameter range we consider here is  $\tilde{\alpha} \lesssim \hbar\omega_0$ ,  $\tilde{B} \ll \hbar\omega_0$ ,  $\tilde{E}_{ac} \ll \hbar\omega_0$ , and we refer to the last condition as the *weak-driving limit*. In the first step, we perform a well-known unitary transformation<sup>5,9</sup> that eliminates the spin-orbit term  $H_{\text{so}}$ , but renders the homogeneous magnetic field inhomogeneous. Second, we express the approximate energy eigenstates of the resulting static Hamiltonian using first-order perturbation theory in the magnetic field. This allows us to identify the basis states of the spin-orbit qubit. Then, we project the complete Hamiltonian, including the driving term  $H_E(t)$ , to this qubit subspace, to reveal the qubit Larmor frequency where resonant excitation is expected, and the Rabi frequency of the qubit Rabi oscillations induced by the electric drive.

The first step is to perform the unitary transformation<sup>5,9</sup>

$$U = e^{i m \alpha z \sigma_y / \hbar} \quad (8)$$

on the Hamiltonian of Eq. (2). This results in the transformed Hamiltonian

$$H'(t) = UH(t)U^\dagger = H'_{\text{osc}} + H'_{\text{so}} + H'_Z + H'_E(t), \quad (9)$$

containing the following terms:

$$H'_{\text{osc}} + H'_{\text{so}} = UH_{\text{osc}}U^\dagger + UH_{\text{so}}U^\dagger = H_{\text{osc}}, \quad (10a)$$

$$H'_Z = UH_ZU^\dagger \quad (10b)$$

$$= -\frac{1}{2} \tilde{B} \left[ \cos\left(\frac{2m\alpha z}{\hbar}\right) \sigma_z + \sin\left(\frac{2m\alpha z}{\hbar}\right) \sigma_x \right],$$

$$H'_E = UH_EU^\dagger = H_E. \quad (10c)$$

Hence the spin-orbit interaction is eliminated and the magnetic field acquires a spiral-type spatial dependence. Note that a position- and spin-independent constant has been omitted in Eq. (10a).

The second step is to express the two lowest-energy eigenstates  $|g'\rangle$  and  $|e'\rangle$  of the transformed static Hamiltonian, using first-order perturbation theory in the Zeeman Hamiltonian. Finally, we project the complete transformed Hamiltonian to the qubit subspace spanned

by  $|g'\rangle$  and  $|e'\rangle$  using the projector  $P = |g'\rangle\langle g'| + |e'\rangle\langle e'|$ . This procedure yields

$$H'_q(t) = PH'(t)P = -\frac{1}{2}\hbar\omega_L\tau_z - \hbar\Omega_R\tau_x\sin(\omega t), \quad (11)$$

where  $\tau_i$  are the Pauli operators in the qubit subspace, e.g.,  $\tau_z = |g'\rangle\langle g'| - |e'\rangle\langle e'|$ . After the rotating-wave approximation<sup>10</sup>, the Schrödinger equation corresponding to  $H'_q$  can be solved exactly. The Larmor frequency is

$$\hbar\omega_L = \tilde{B}e^{-2\left(\frac{\tilde{\alpha}}{\hbar\omega_0}\right)^2}, \quad (12)$$

which describes the spin-orbit-induced suppression of the Zeeman splitting<sup>5</sup>, and the Rabi frequency upon resonant driving  $\omega = \omega_L$  is<sup>5-7</sup>.

$$\Omega_R = \frac{2\tilde{E}_{ac}\tilde{\alpha}}{(\hbar\omega_0)^2}\omega_L. \quad (13)$$

In this resonant case the qubit can be flipped from its ground state to its excited state, so the excited-state population  $P_e$  shows simple Rabi oscillations:

$$P_e(\tau) = \sin^2(\Omega_R\tau/2). \quad (14)$$

#### IV. PRACTICAL CONSIDERATIONS AND ESTIMATES

As stated in the introduction, the main questions we address here are as follows. Given certain practical constraints, how fast can we perform a single qubit flip? What is the corresponding drive strength required for that fast flip? How do these quantities depend on the tunable parameters?

We can develop naive answers to these questions based on the analytical results (12) and (13) obtained for the weak-driving limit. As it was discussed in section I, the pulses have a duration  $\tau = N\pi/\omega$ , and in the resonant case is

$$\tau = N\pi/\omega_L. \quad (15)$$

The shortest pulse duration corresponds to a single half-cycle, that is, to the  $N = 1$  case. For a qubit flip, the driving amplitude should fulfill  $P_e(\tau) = 1$ , that is,  $\Omega_R\tau/2 = \pi/2$ . From this condition, using Eq. (13), we obtain that the drive strength corresponding to the shortest qubit-flip pulse is

$$\tilde{E}_{ac} = \frac{(\hbar\omega_0)^2}{2n\tilde{\alpha}}. \quad (16)$$

It is important to note that the result (16) is naive in the sense that the results (13) and (14) are established only in the weak-driving limit,  $\tilde{E}_{ac} \ll \hbar\omega_0$ , whereas a parameter set fulfilling Eq. (16), may lie outside this parameter regime. For example, if  $N = 1$ ,  $\tilde{\alpha}/\hbar\omega_0 = 0.5$ , then the drive strength from Eq. (16) is  $\tilde{E}_{ac} = \hbar\omega_0$  which contradicts the weak-driving condition  $\tilde{E}_{ac} \ll \hbar\omega_0$ . (Note

that this choice of  $\tilde{\alpha}/\hbar\omega_0$  maximizes the Rabi frequency as the function of spin-orbit strength, see Eqs. (12) and (13).)

In the rest of this work, we study the qubit-flip processes induced by strong driving, in the range  $\tilde{E}_{ac} \lesssim \hbar\omega_0$ . Surprisingly, as we show in Section V, we find that the characteristics of the fast qubit-flips induced by half-cycle driving are rather well described by naively extrapolating the results (15) and (16) obtained for the weakly driven case. First we present an analytical derivation, then we compare it to the numerical simulations in Sec. V and in Sec. VI.

Anticipating that the extrapolation of the weak-driving results gives an accurate description of the strongly driven case, here we use it to draw practical conclusions. If our goal is to achieve qubit-flips as fast as possible, i.e., to minimize  $\tau$ , then Eq. (15) advises to set the Larmor frequency as high as possible. Practically, one upper bound on the Larmor frequency is given by the maximal achievable magnetic field strength. Another upper bound follows from the resonant-driving condition: the maximal Larmor frequency is limited by the maximum available driving frequency.

For the sake of a practical example, assume that the maximum available driving frequency is  $\omega_{\max}/(2\pi) = 50$  GHz. Furthermore, consider an InAs nanowire quantum dot<sup>1,4</sup> with electronic effective mass  $m = 0.023m_0$ , effective g-factor  $g^* = 10$ , orbital level spacing  $\hbar\omega_0 = 1$  meV, and spin-orbit strength  $\alpha = 62$  km/s. These parameters imply an electronic confinement length  $L = \sqrt{\hbar/(m\omega_0)} \approx 58$  nm.

In this case, the magnetic field strength corresponding to  $\omega_L = \omega_{\max}$  is  $B \approx 0.6$  T, which is experimentally feasible. Hence, in this case, the component limiting the achievable qubit-flip speed is the limited driving frequency. In this example, Eq. (15) predicts that the shortest achievable qubit-flip takes  $\tau = 10$  ps, which is 3 orders of magnitude shorter than the 10 ns qubit-flip time scale demonstrated experimentally in Ref. 1. To achieve this, the driving amplitude should be set to  $\tilde{E}_{ac} = \hbar\omega_0$ , corresponding to a driving field amplitude  $E_{ac} \approx 25$  kV/m, and an electron oscillation amplitude  $A = \frac{\sqrt{2}\tilde{E}_{ac}}{\hbar\omega_0}L \approx 82$  nm.

#### V. STRONG DRIVING DESCRIBED IN THE CO-MOVING FRAME

Having established the weakly driven spin dynamics in Sec. III, it is natural to ask how this dynamics changes if the drive strength is not perturbative, i.e., if we do not assume  $\tilde{E}_{ac} \ll \hbar\omega_0$  but allow for  $\tilde{E}_{ac} \lesssim \hbar\omega_0$  instead?

As we already noted above, the analytical results Eqs. (12) and (13) and the corresponding dynamics is recovered to a large extent in the strong-driving case. Our strategy to obtain an analytical description of the strongly driven qubit dynamics is as follows. As the first step, following the perturbative case in Section III, we

apply the transformation  $U$  of Eq. (8) on our Hamiltonian  $H$  to eliminate spin-orbit interaction at the price of rendering the magnetic field inhomogeneous. Then, we transform to a spatial reference frame that is co-moving with the center of the time-dependent harmonic oscillator potential  $\frac{1}{2}m\omega_0^2 z^2 + eE_{\text{ac}}z \sin(\omega t)$ , and to a spin reference frame which is co-moving with the local magnetic field at the center of the confinement potential. These transformations then allow us to focus again on a two-dimensional low-energy effective qubit subspace that is sufficiently decoupled from higher-lying energy eigenstates, and thereby to deduce analytical results for the qubit dynamics.

The first transformation,  $U$  results in the Hamiltonian terms collected in Eq. (10). The second transformation, i.e., the spatial transformation to the co-moving frame<sup>11–13</sup>, is described by the time-dependent unitary operator

$$W(t) = \sum_{n=0}^{\infty} |n\rangle \langle n(t)|, \quad (17)$$

where  $|n\rangle$  is the  $n$ th eigenstate of the undriven harmonic oscillator  $H_{\text{osc}}$ , and  $|n(t)\rangle$  is the instantaneous eigenstate of the driven harmonic oscillator  $H_{\text{osc}} + H_E(t)$ . Note that an alternative way to express this transformation is

$$W(t) = e^{-iA \sin(\omega t) p_z / \hbar}. \quad (18)$$

This time-dependent unitary transformation results in the transformed Hamiltonian

$$\begin{aligned} H''(t) &= W(t)H'(t)W^\dagger(t) + i\hbar\dot{W}(t)W^\dagger(t) \\ &= H_{\text{osc}} + H'_Z(z - A \sin \omega t) + A\omega \cos(\omega t)p_z \end{aligned} \quad (19)$$

The first two terms of Eq. (19) describes an electron in a static harmonic confinement subject to an inhomogeneous spiral-like, oscillating Zeeman field. As the final, third transformation, we eliminate the time dependence of the inhomogeneous Zeeman field via the time-dependent spin-rotating unitary transformation

$$S(t) = e^{-i \frac{m\alpha A \sin(\omega t)}{\hbar} \sigma_y}. \quad (20)$$

This yields

$$\begin{aligned} H'''(t) &= S(t)H''(t)S^\dagger(t) + i\hbar\dot{S}(t)S^\dagger(t) \\ &= H_{\text{osc}} + H'_Z(z) + A\omega \cos(\omega t)p_z \\ &\quad + Am\alpha\omega \cos(\omega t)\sigma_y. \end{aligned} \quad (21)$$

This result is useful: even in the range of strong spin-orbit interaction  $\tilde{\alpha} \sim \hbar\omega_0$  and strong driving  $\tilde{E}_{\text{ac}} \sim \hbar\omega_0$ , the qubit Hamiltonian obtained by projecting  $H'''(t)$  to the lowest-energy two-dimensional subspace provides an accurate description of the dynamics. Using the projector  $Q = |0 \uparrow\rangle \langle 0 \uparrow| + |0 \downarrow\rangle \langle 0 \downarrow|$ , the qubit Hamiltonian reads

$$\begin{aligned} H_q'''(t) &= QH'''(t)Q \\ &= -\frac{1}{2}\hbar\omega_L\sigma_z + Am\alpha\omega \cos(\omega t)\sigma_y. \end{aligned} \quad (22)$$

where the first, static term is the contribution from the inhomogeneous Zeeman term  $H'_Z(z)$  in Eq. (21),  $\omega_L$  is given by Eq. (11), and the second, driving term is the contribution from the fourth term in Eq. (21). Note that the arrows in the above definition of  $Q$  do not correspond to the physical spin degree of freedom, since we have performed spin-dependent unitary transformations along the way. Note also that the dynamics in the qubit subspace is coupled to the higher-lying energy levels via  $H'_Z(z)$  and the  $p$ -linear term in Eq. (21), but the corresponding coupling matrix elements are weak compared to the level spacing  $\hbar\omega_0$  as long as  $\tilde{\alpha}, \tilde{E}_{\text{ac}} \lesssim \hbar\omega_0$  and the Zeeman splitting is small compared to the orbital level spacing,  $\omega_L \ll \omega_0$ .

In conclusion, with our result Eq. (22), we have established that even in the nonperturbative regime of strong spin-orbit interaction and strong driving, the qubit can be described in an appropriately chosen reference frame as a simple harmonically driven two-level system. Furthermore, a comparison of Eq. (11) and (22) reveals that the analytical results for the qubit Larmor frequency is the same for the strong-driving case ( $\tilde{E}_{\text{ac}} \sim \hbar\omega_0$ ) as for the weak-driving case ( $\tilde{E}_{\text{ac}} \ll \hbar\omega_0$ ). Even more, the Rabi frequency upon resonant drive is also described by the same formula in the two cases: this is seen if the prefactor  $Am\alpha\omega$  in Eq. (22) is evaluated using the resonance condition  $\omega = \omega_L$  and expressed via the parameters  $\tilde{E}_{\text{ac}}$ ,  $\tilde{\alpha}$ , and the resulting driving Hamiltonian is compared to Eq. (11). Therefore, our analysis in this section have shown that the results obtained for the weakly driven case can simply be extrapolated to the strong-driving regime.

## VI. FAST SPIN FLIP DUE TO STRONG HALF-CYCLE EXCITATION

In this section, we solve the time-dependent Schrödinger equation to investigate the accuracy of the analytical results derived in the preceding section.

First, we outline the procedure to obtain numerical results for the dynamics. The first step is to expand the Hamiltonian (21) in the first  $n_{\text{max}}$  harmonic oscillator eigenstates. Due to the spin degree of freedom, the size of this truncated Hamiltonian matrix is  $2n_{\text{max}} \times 2n_{\text{max}}$ . Second, the initial state in this time-dependent frame is  $|g'''\rangle$ , which the state obtained via transforming the lab-frame ground state  $|g\rangle$  of the spin-orbit qubit with the three transformations discussed above:  $|g'''\rangle = S(t=0)W(t=0)U|g\rangle$ . Note that both  $S(t=0)$  and  $W(t=0)$  are identity operators (actually, they are identity operators for any  $t = N\pi/\omega$ ), which implies  $|g'''\rangle = |g\rangle$ , hence we obtain the initial state by diagonalizing the static part of  $H'(t)$ . Third, we numerically solve the time-dependent Schrödinger equation governed by  $H'''(t)$  to obtain the time evolution  $|\psi'''(t)\rangle$  of the initial state. Fourth, we transform the solution back to the frame of  $H'$  via  $|\psi'(t)\rangle = W^\dagger(t)S^\dagger(t)|\psi'''(t)\rangle$ . Fifth, we evaluate



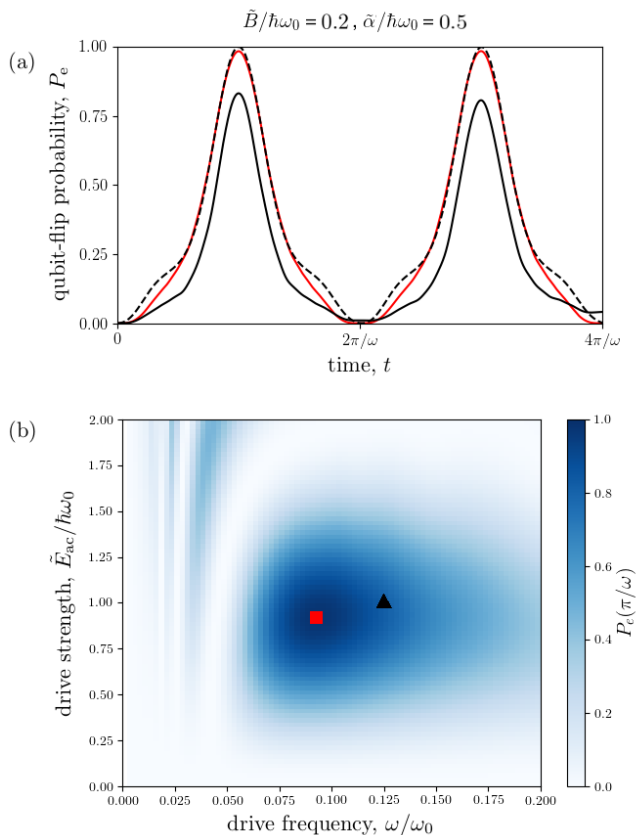


FIG. 2. **Qubit-flip probability of a spin-orbit qubit due to a half-cycle electric excitation.** (a) Black solid line shows the numerical result for qubit-flip probability  $P_e(t)$ , for drive frequency  $\omega \approx 0.121\omega_0$  and  $\tilde{E}_{ac} = \hbar\omega_0$  corresponding to the black triangle in (b). For these parameters, the analytical result (dashed black line) predicts a perfect qubit flip at  $t = \pi/\omega$ . Red line: qubit-flip probability for parameter values  $\omega \approx 0.092\omega_0$  and  $\tilde{E}_{ac} = 0.916\hbar\omega_0$ , corresponding to the red square in (b). (b) Numerical results for the qubit-flip probability after a half cycle,  $P_e(\pi/\omega)$ , as a function of  $\omega$  and  $\tilde{E}_{ac}$ . Red square marks the maximum of the qubit-flip probability.

the qubit-flip probability via  $P_e(t) = |\langle e' | \psi'(t) \rangle|^2$ .

Solving the time-dependent Schrödinger equation in the co-moving frame is computationally more efficient than doing that in the lab frame. For the co-moving frame, as we increase the number  $n_{\max}$  of harmonic oscillator basis states, the qubit-flip probability  $P_e(t)$  converges rapidly. For the parameter set discussed below, the choice  $n_{\max} = 4$  already provides satisfactory convergence. To have the same accuracy from a lab-frame simulation, we need a significantly larger basis  $n_{\max} = 10$ .

In addition to the numerical approach, we can also describe the driven qubit dynamics using an analytical approximation. This is based on the effective qubit Hamiltonian  $H_q'''(t)$  in Eq. (22). We take the initial state as the ground state of the static part of  $H_q'''(t)$ , assume that the dynamics described by the wave function  $|\psi'''(t)\rangle$  is restricted to this two-dimensional qubit

subspace, and within this subspace it follows the simple Rabi dynamics according to the rotating-wave approximation. Again, the qubit-flip probability is obtained via  $P_e(t) = |\langle e' | W^\dagger(t) S^\dagger(t) \psi'''(t) \rangle|^2$ , where  $|e'\rangle$  is obtained perturbatively, as described in Section III.

Here we will discuss certain features of the driven qubit time evolution in the case of strong driving  $\tilde{E}_{ac} \sim \hbar\omega_0$ , when the amplitude  $A = \frac{\sqrt{2}\tilde{E}_{ac}}{\hbar\omega_0}L$  of the real-space oscillations of the electronic wave function is comparable to the width  $L$  of the wave function. Note that a priori we do not expect that the numerical solution will show simple Rabi-oscillation qubit dynamics under this strong-driving condition. In fact, it is known that even in simple magnetic resonance with a spin-1/2, an increased driving strength leads to unconventional dynamics<sup>6,10,14–16</sup>.

Hence the first question we address is whether a high-quality qubit-flip is achievable with a strong half-cycle excitation pulse? Consider the example when the magnetic field and the spin-orbit strength are set as  $\tilde{B} = 0.2\hbar\omega_0$  and  $\tilde{\alpha} = 0.5\hbar\omega_0$ . For this setting, the results (12), (15), and (16) suggest that the fastest qubit-flip is achievable by a strong half-cycle pulse ( $N = 1$ ) with resonant drive frequency  $\omega = \omega_L \approx 0.121\omega_0$  and drive strength  $\tilde{E}_{ac} = \hbar\omega_0$ . The analytical (numerical) time evolution of the qubit-flip probability  $P_e(t)$  is shown for this parameter set in Fig. 2a as a dashed (solid) black line. On the one hand, the comparison of the two results reveals that the actual dynamics (solid) deviates from the analytical approximation (dashed). On the other hand, we also see that a fairly high qubit-flip probability  $P_e \approx 0.8$  is achieved at  $t = \pi/\omega$ .

The latter observation suggests that a high-fidelity qubit flip may be achieved with a strong half-cycle pulse by slightly adjusting the drive parameters. To explore this possibility, we extend the numerical simulations of the qubit dynamics to a range of values of drive frequency  $\omega$  and drive strength  $\tilde{E}_{ac}$ . We plot the qubit-flip probability  $P_e(\pi/\omega)$  at the end of a half-cycle excitation as a function of these parameters in Fig. 2b; there the black triangle corresponds to the black solid curve of Fig. 2a discussed above. In Fig. 2b, the highest qubit-flip probability is found in the point marked with the red square, where  $P_e(\pi/\omega) \approx 0.98$ . The corresponding complete time evolution  $P_e(t)$  is shown as the red curve in Fig. 2a. These results demonstrate that even though the qubit-flip probability  $P_e(t)$  is more complex than a simple Rabi oscillation (14) in case of a strong half-cycle drive, a high-fidelity qubit flip can still be reached by fine tuning the parameters of the drive.

Recall that the considerations in Sec. IV, especially Eq. (15), suggest that the qubit flip can be made faster by increasing the Larmor frequency via increasing the magnetic field. To test this expectation, we extend the numerical investigation to a range of magnetic field values, and report the results in Fig. 3. For each value of the magnetic field, we compute the qubit-flip probability  $P_e(\pi/\omega; \omega, \tilde{E}_{ac})$  upon a half-cycle pulse, and maximize  $P_e(\pi/\omega)$  with respect to  $\omega$  and  $\tilde{E}_{ac}$ . This maximum

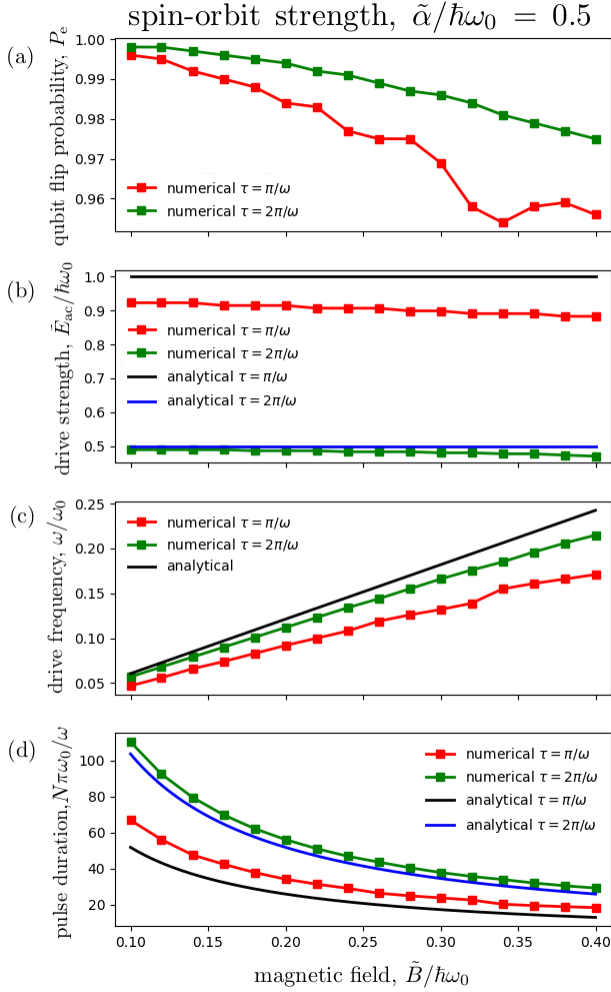


FIG. 3. **Magnetic field dependence of qubit-flip pulse parameters.** (a) Numerically computed maximal qubit-flip probability after a half-cycle (red) or single-cycle (green) drive pulse. (b,c,d) The drive strength  $\tilde{E}_{ac}$ , drive frequency  $\omega$ , and pulse duration  $\tau$ , corresponding to the maxima of  $P_e$  shown in (a). Solid lines show the analytical results.

point for a certain magnetic-field value was shown as the red square in Fig. 2b. Red squares in Fig. 3a show the maximal qubit-flip probability found by this procedure as function of magnetic field, and in Figs. 3b and c, the drive strength  $\tilde{E}_{ac}$  and drive frequency  $\omega$  corresponding to this maximum. In Fig. 3b and c the black solid line shows the analytical result Eq. (16) and (12) respectively. In Fig. 3d, red squares and black line show the pulse duration  $\tau = \pi/\omega$ , derived directly from the data in Fig. 3c.

The main conclusions drawn from Fig. 3 are as follows. (i) Fig. 3d confirms the expectation that a larger magnetic field allows for a faster qubit flip. (ii) Even though faster qubit flips can be achieved by increasing the magnetic field, the numerical data (red squares) in Fig. 3b confirms that the drive strength does not have

to be increased to achieve that. (iii) The qubit flips are not perfect: Fig. 3a shows that the larger the magnetic field, the smaller the maximal qubit-flip probability. This is important if this qubit-flip process is considered in the context of quantum information processing: the result suggests that by increasing the magnetic field, a faster, but less precise quantum-logical operation is realized. (iv) The trends and orders of magnitude predicted by the estimates in Sec. IV (black solid lines in Fig. 3) are confirmed by the numerical data (red squares in Fig. 3), although there are quantitative deviations of a few tens of percents.

Experimental constraints might inhibit the application of a half-cycle pulse: it might be challenging to produce such a strong electric field, or if realized, the strong field could ionize the quantum dot. This motivates to consider the case when a drive pulse with the duration of a few half-cycles is applied. For example, Eq. (16) suggests that the drive strength required for a single-cycle pulse ( $N = 2$ ,  $\tau = 2\pi/\omega$ ) is half of the drive strength of the half-cycle pulse; this is shown as the blue line in Fig. 3b. The corresponding numerical result (green squares) confirms this. Note that Fig. 3a shows that the precision of the qubit-flip improves by using a single-cycle pulse instead of a half-cycle one. This is expected, as the qubit dynamics is expected to approach the simple Rabi dynamics as the drive strength is reduced. Finally, since the half-cycle and single-cycle pulses are both approximately resonant with the qubit Larmor frequency, the latter one is half as fast as the former one, which is also seen in Fig. 3d.

Our results discussed in this section are all phrased in terms of dimensionless parameters; here we make connection to realistic parameter values. Again we take the example of an InAs quantum dot, with parameters specified in Sec. IV. Then the dimensionless parameters  $\tilde{B}/\hbar\omega_0 = 0.2$ ,  $\tilde{E}_{ac}/\hbar\omega_0 = 0.916$ ,  $\omega/\omega_0 = 0.092$  corresponding to the red square in Fig. 2 are translated to magnetic field  $B = 0.35$  T, drive strength  $E_{ac} = 22$  kV/m, (or oscillation amplitude  $A = 75$  nm) and drive frequency  $\omega/2\pi = 22$  GHz.

## VII. DISCUSSION AND CONCLUSIONS

### *Effect of the spin-orbit strength on the qubit-flip time.*

In Sec. VI, we considered a fixed spin-orbit strength  $\tilde{\alpha}$ , and concluded that the qubit-flip time can be shortened by increasing the magnetic field. However, the spin-orbit strength is also tunable experimentally<sup>17–20</sup>. Therefore, a complementary question concerns the case of a fixed magnetic field: how does the qubit-flip time depend on the strength of the spin-orbit interaction? In the absence of any practical constraints, a simple and slightly counterintuitive answer can be based on the naive estimates in Sec. IV: the qubit-flip time can be reduced by reducing the spin orbit strength. This is a consequence of the fact that in our model, the qubit Larmor frequency increases when the spin-orbit strength is re-

duced (see Eq. (12)), and therefore the duration of a resonant half-cycle pulse gets shorter. Our numerical simulation results (not shown) do confirm this expectation. A practical constraint is the following. By reducing the spin-orbit strength, the drive strength  $\tilde{E}_{ac}$  required for the qubit flip grows, according to Eq. (16). In an actual device, the drive strength corresponding to the ionization of the quantum dot cannot be exceeded, which implies a minimal value of the spin-orbit strength. That minimal spin-orbit strength provides a lower bound on the qubit flip time, and there is no practical advantage of going below that minimal spin-orbit strength.

*Further directions.* We have been focusing on the gross features of the dynamics of spin-orbit qubits induced by strong electric fields. A further, more refined analysis is motivated by the potential application of this setup in quantum information processing; that should incorporate a more generic description of the spin-orbit interaction, the investigation of quantum-gate fidelities, realistic and optimized electric pulse shapes beyond the harmonic-driving paradigm, as well as decoherence processes. We think that the numerical and analytical methods we developed here, based on the co-moving frame transformation, will serve as useful tools for addressing such extensions.

*Conclusions.* In this work, we have described the elec-

trically driven dynamics of a spin-orbit qubit, in the regime of strong driving, when the amplitude of spatial oscillations of the electron are comparable to the width of its wave function. Using the model of a one-dimensional quantum dot subject to Rashba spin-orbit interaction, we have demonstrated that strong electric pulses with short duration allow for fast, high-precision qubit control, potentially on the sub-nanosecond time scale. Our analysis of the dependence of the shortest achievable qubit-flip time scale on experimentally tunable parameters (magnetic field, spin-orbit strength) offers practical guidelines to optimize electrically induced single-qubit operations on spin-orbit qubits.

## ACKNOWLEDGMENTS

We thank P. Boross and G. Széchenyi for useful feedback on the manuscript. This research was supported by the National Research Development and Innovation Office of Hungary within the Quantum Technology National Excellence Program (Project No. 2017-1.2.1-NKP-2017-00001). AP acknowledges funding from the NKFIH Grants 105149 and 124723, and the New National Excellence Program of the Ministry of Human Capacities of Hungary.

- 
- <sup>1</sup> S. Nadj-Perge, S. M. Frolov, and L. P. Kouwenhoven, "Spin-orbit qubit in a semiconductor nanowire," *Nature*, vol. 468, pp. 1084–1087, Dec 2010.
  - <sup>2</sup> K. C. Nowack, F. H. L. Koppens, Y. V. Nazarov, and L. M. K. Vandersypen, "Coherent Control of a Single Electron Spin with Electric Fields," *Science*, vol. 318, no. 5855, pp. 1430–1433, 2007.
  - <sup>3</sup> S. Nadj-Perge, V. S. Pribiag, J. W. G. van den Berg, K. Zuo, S. R. Plissard, E. P. A. M. Bakkers, S. M. Frolov, and L. P. Kouwenhoven, "Spectroscopy of Spin-Orbit Quantum Bits in Indium Antimonide Nanowires," *Phys. Rev. Lett.*, vol. 108, p. 166801, Apr 2012.
  - <sup>4</sup> M. D. Schroer, K. D. Petersson, M. Jung, and J. R. Petta, "Field Tuning the  $g$  Factor in InAs Nanowire Double Quantum Dots," *Phys. Rev. Lett.*, vol. 107, p. 176811, Oct 2011.
  - <sup>5</sup> R. Li, J. You, C.P.Sun, and F. Nori, "Controlling a Nanowire Spin-Orbit Qubit via Electric-Dipole Spin Resonance," *Physical Review Letters*, vol. 111, pp. 086805–1–086805–5, 2013.
  - <sup>6</sup> J. Romhányi, G. Burkard, and A. Pályi, "Subharmonic transitions and Bloch-Siegert shift in electrically driven spin resonance," *Phys. Rev. B*, vol. 92, p. 054422, Aug 2015.
  - <sup>7</sup> V. N. Golovach, M. Borhani, and D. Loss, "Electric-dipole-induced spin resonance in quantum dots," *Phys. Rev. B*, vol. 74, p. 165319, Oct 2006.
  - <sup>8</sup> C. Flindt, A. S. Sørensen, and K. Flensberg, "Spin-Orbit Mediated Control of Spin Qubits," *Phys. Rev. Lett.*, vol. 97, p. 240501, Dec 2006.
  - <sup>9</sup> L. S. Levitov and E. I. Rashba, "Dynamical spin-electric coupling in a quantum dot," *Phys. Rev. B*, vol. 67, p. 115324, Mar 2003.
  - <sup>10</sup> J. H. Shirley, "Solution of the Schrödinger Equation with a Hamiltonian Periodic in Time," *Phys. Rev.*, vol. 138, pp. B979–B987, May 1965.
  - <sup>11</sup> E. A. Laird, C. Barthel, E. I. Rashba, C. M. Marcus, M. P. Hanson, and A. C. Gossard, "Hyperfine-mediated gate-driven electron spin resonance," *Phys. Rev. Lett.*, vol. 99, p. 246601, Dec 2007.
  - <sup>12</sup> E. A. Laird, C. Barthel, E. I. Rashba, C. M. Marcus, M. P. Hanson, and A. C. Gossard, "A new mechanism of electric dipole spin resonance: hyperfine coupling in quantum dots," *Semiconductor Science and Technology*, vol. 24, no. 6, p. 064004, 2009.
  - <sup>13</sup> G. Széchenyi and A. Pályi, "Maximal Rabi frequency of an electrically driven spin in a disordered magnetic field," *Phys. Rev. B*, vol. 89, p. 115409, Mar 2014.
  - <sup>14</sup> F. Bloch and A. Siegert, "Magnetic Resonance for Nonrotating Fields," *Phys. Rev.*, vol. 57, pp. 522–527, Mar 1940.
  - <sup>15</sup> G. D. Fuchs, V. V. Dobrovitski, D. M. Toyli, F. J. Heremans, and D. D. Awschalom, "Gigahertz dynamics of a strongly driven single quantum spin," *Science*, vol. 326, p. 1520, 2009.
  - <sup>16</sup> Y.-C. Yang, S. N. Coppersmith, and M. Friesen, "Achieving high-fidelity single-qubit gates in a strongly driven silicon-quantum-dot hybrid qubit," *Phys. Rev. A*, vol. 95, p. 062321, Jun 2017.
  - <sup>17</sup> S. Dhara, H. S. Solanki, V. Singh, A. Narayanan, P. Chaudhari, M. Gokhale, A. Bhattacharya, and M. M. Deshmukh, "Magnetotransport properties of individual InAs nanowires," *Phys. Rev. B*, vol. 79, p. 121311, Mar 2009.

- <sup>18</sup> I. van Weperen, B. Tarasinski, D. Eeltink, V. S. Pribiag, S. R. Plissard, E. P. A. M. Bakkers, L. P. Kouwenhoven, and M. Wimmer, “Spin-orbit interaction in InSb nanowires,” *Phys. Rev. B*, vol. 91, p. 201413, May 2015.
- <sup>19</sup> D. Liang and X. P. Gao, “Strong Tuning of Rashba SpinOrbit Interaction in Single InAs Nanowires,” *Nano Letters*, vol. 12, no. 6, pp. 3263–3267, 2012. PMID: 22545669.
- <sup>20</sup> Z. Scherübl, G. m. H. Fülöp, M. H. Madsen, J. Nygård, and S. Csonka, “Electrical tuning of Rashba spin-orbit interaction in multigated InAs nanowires,” *Phys. Rev. B*, vol. 94, p. 035444, Jul 2016.